

# Hyaluronic Acid-Based Microgels and Microgel Networks for Vocal Fold Regeneration

Xinqiao Jia,<sup>\*,†</sup> Yoon Yeo,<sup>‡</sup> Rodney J. Clifton,<sup>§</sup> Tong Jiao,<sup>§</sup> Daniel S. Kohane,<sup>||</sup>  
James B. Kobler,<sup>⊥</sup> Steven M. Zeitels,<sup>⊥</sup> and Robert Langer<sup>‡</sup>

*Department of Materials Science and Engineering, 201 DuPont Hall, University of Delaware, Newark, Delaware 19716, Department of Chemical Engineering, E25/342, Massachusetts Institute of Technology, 77 Massachusetts Avenue, Cambridge, Massachusetts 02139, Division of Engineering, Box D, Brown University, Providence, Rhode Island 02912, and Pediatric Intensive Care Unit and Center for Laryngeal Surgery & Voice Rehabilitation, Massachusetts General Hospital, Harvard Medical School, Boston, Massachusetts 02114*

*Received May 19, 2006; Revised Manuscript Received September 7, 2006*

Vocal fold scarring disrupts the viscoelastic properties of the lamina propria that are critical for normal phonation. There is a clinical need for the development of advanced biomaterials that approximate the mechanical properties of the lamina propria for in vivo vocal fold regeneration. We have developed hyaluronic acid (HA)-based microgels and cross-linked microgel networks with tunable degradation and mechanical properties. HA microgels were prepared by cross-linking HA derivatives carrying hydrazide (HAADH) and aldehyde (HAALD) functionalities within the inverse emulsion droplets. Alternatively, poly(ethylene glycol) dialdehyde (PEGDiALD) was employed in place of HAALD. Microgels based on HAADH/HAALD are more resistant to enzymatic degradation than those generated from HAADH/PEGDiALD. In vitro cytotoxicity studies using vocal fold fibroblasts indicate that microgels synthesized from HAADH/HAALD are essentially nontoxic, whereas microgels derived from HAADH/PEGDiALD exhibit certain adverse effects on the cultured cells at high concentration ( $\geq 2$  mg/mL). These microgels exhibit residual functional groups that can be used as reactive handles for covalent conjugation of therapeutic molecules. The presence of residual functional groups also allows for subsequent cross-linking of the microgels with other reactive polymers, giving rise to doubly cross-linked networks (DXNs) with tunable viscoelasticity. Mechanical measurements using a torsional wave apparatus indicate that HA-based DXNs exhibit elastic moduli that are similar to those of vocal fold lamina propria at frequencies close to the range of human phonation. These HA-based microgel systems are promising candidates for the treatment of vocal fold scarring, not just as biocompatible filler materials, but as smart entities that can repair focal defects, smooth the vocal fold margin, and potentially soften and dissolve scar tissue.

## Introduction

Vocal folds are located side by side in the larynx just above the trachea. In humans, each fold is roughly 10–15 mm in length and 5 mm thick. Histologically, the vocal fold is a laminated structure consisting of a stratified squamous epithelium, lamina propria (LP), and vocalis muscle.<sup>1,2</sup> A great variety of sounds are produced when the vocal folds are blown apart into entrained vibration by the tracheal air stream. Under normal conditions, vocal folds can sustain up to 60% strain at frequencies of 75–1000 Hz.<sup>3</sup> However, mechanical stresses from excessive phonation and deleterious environmental factors such as smoke, alcohol, and refluxed stomach acid can cause damage to this delicate system, resulting in basement-membrane-zone phonotrauma in the superficial lamina propria (SLP).<sup>4</sup> This phonotrauma morphologically presents as nodules, polyps,

ectasias, varices, and sulcus deformities at the medial surface of the vocal folds.<sup>5</sup>

The phonatory epithelium encapsulates the SLP to comprise the mucosa, which has long been noted to be the key layer for vibration.<sup>6</sup> Diminished vocal fold mucosal pliability is the primary etiology of most human hoarseness.<sup>7</sup> Therefore, the SLP is the key target for restoration. Although precision phonomicrosurgery is quite successful for benign mass lesions of the vocal folds,<sup>5,8</sup> these techniques would be enhanced by SLP substitutes or tissue-engineered SLP grafts.<sup>7</sup> Accordingly, there is a clinical need for the development of advanced biomaterials that approximate the biomechanical properties of the SLP and can be directly injected to treat vocal fold scarring.<sup>5,9,10</sup>

The search for injectable vocal fold biomaterials has largely focused on derivatives of hyaluronic acid (HA).<sup>9,10</sup> HA is an important extracellular matrix (ECM) component of the LP. It contributes to the maintenance of an optimal tissue viscosity to facilitate phonation and an optimal tissue stiffness that may be important in determining vocal fundamental frequency.<sup>11</sup> It has been suggested that if there are lower amounts of HA in the most superficial area of the LP, there is less protection from vibratory trauma and overuse.<sup>12</sup> In addition, examination of the HA levels in a rabbit animal model indicated that HA levels were significantly lower up to day 15 following vocal fold stripping.<sup>13</sup> These studies suggest that local enrichment of HA

\* To whom correspondence should be addressed. Phone: (302) 831-6553. Fax: (302) 831-4545. E-mail: xjia@udel.edu.

<sup>†</sup> University of Delaware.

<sup>‡</sup> Massachusetts Institute of Technology.

<sup>§</sup> Brown University.

<sup>||</sup> Pediatric Intensive Care Unit, Massachusetts General Hospital, Harvard Medical School.

<sup>⊥</sup> Center for Laryngeal Surgery & Voice Rehabilitation, Massachusetts General Hospital, Harvard Medical School.

may provide useful strategies for vocal fold repair. Because native HA has a short half-life in vivo,<sup>14</sup> chemically cross-linked HA hydrogels have been synthesized<sup>15,16</sup> and evaluated for their potential to treat vocal fold scarring.<sup>9,17–21</sup> HA–collagen composite hydrogels have been applied for in vitro culturing of vocal fold fibroblasts.<sup>22</sup>

Despite some promising results with cross-linked HA hydrogels, there are inherent challenges in the use of bulk hydrogels. One disadvantage is that degradation profiles and mechanical properties cannot be adjusted without adversely affecting each other. Stiffer gels may be more resistant to degradation but also may be too stiff to vibrate optimally.<sup>23</sup> A second shortcoming is that tissue integration may be poor due to the limited surface area. Finally, bulk hydrogels also suffer from their inability to recover from mechanical stress, leading to altered viscoelasticity over time after implantation.

To overcome these limitations, we have created a new class of vocal fold implant materials based on HA microgels. We hypothesized that individual microgels can be highly cross-linked, making them resistant to degradation, while macroscale mechanical properties might be independently tunable by adjusting the microgel dimensions or intermicrogel cross-linking. Moreover, the microgels have a relatively large surface area, which might improve tissue integration and facilitate controlled delivery of therapeutics. Finally, the presence of two levels of cross-linking (within and between individual microgels) may offer potential for rapid recovery from mechanical stress.

Recently there has been an increasing interest in HA-based microparticle formulations for drug<sup>24,25</sup> or cell<sup>26</sup> delivery applications. While most studies focus on hard particulate systems based on esterified derivatives of HA that are insoluble in aqueous conditions,<sup>24</sup> efforts are also directed toward engineering soft hydrogel particles (microgels) using water-soluble HA precursors that can be covalently cross-linked.<sup>25,26</sup> However, in these previous studies, the microgels were prepared in such a way that the residual reactants<sup>25</sup> or the unwanted component<sup>26</sup> had to be removed afterward, which makes the preparation procedures rather cumbersome and leaves toxicity concerns.

Here, we report HA-based microgels prepared by in situ cross-linking of chemically modified HAs within inverse emulsion droplets. These microgels exhibit benign cellular responses, improved enzymatic stability, and defined functionality. Macroscopic hydrogels with tunable viscoelasticity can be readily obtained by further cross-linking with soluble macromolecules through the residual functional groups on microgel surfaces, leading to a doubly cross-linked network (DXN) with hierarchical organization. We hope with further study, these DXNs will lead to promising treatment for vocal fold scarring.

## Experimental Section

**Materials.** HA (sodium salt,  $M_w = 1.3$  MDa or 490 KDa) was purchased from Genzyme Corp. (Cambridge, MA). Bovine testicular hyaluronidase (Haase; 30000 U/mg) was obtained from Sigma (St. Louis, MO). Adipic dihydrazide (ADH), 1-ethyl-3-[3-(dimethylamino)propyl]carbodiimide (EDC), sodium hydroxide, and hydrochloric acid were obtained from Aldrich (Milwaukee, WI). 1-Hydroxybenzotriazole (HOBt) was purchased from Alfa Aesar (Ward Hill, MA). Lucifer yellow (LY; potassium salt) was purchased from Molecular Probes (Carlsbad, CA). Hexanes and isopropyl alcohol were obtained from VWR International (West Chester, PA). Poly(ethylene glycol) dialdehyde (PEGDiALD; MW = 3400, percent substitution 96%) was obtained from Nektar Therapeutics (San Carlos, CA). Fresh porcine vocal folds (6–12 months old) were obtained from Research 87 Inc. (Boylston, MA). All tissue culture media and serums were purchased

from Invitrogen (Carlsbad, CA). The MTT cell proliferation assay kit was purchased from ATCC (Manassas, VA). Other chemicals were from Aldrich and were used without further purification.

**Chemical Modification of HA.** Chemical modification of HA was carried out in aqueous conditions following previously described procedures.<sup>27,28</sup> Briefly, periodate oxidation was applied to generate HA with varying percentages of dialdehyde content (16%, 39%, and 70% as determined by the modified TNBS assay<sup>21,29</sup>). The resulting polymers are designated as HAALD16, HAALD39, and HAALD70, respectively. To obtain HA derivatives with comparable molecular weights, the oxidation reaction was carried out using HA with  $M_w = 1.3$  MDa, while the carbodiimide-mediated reaction between ADH and HA was conducted using HA with  $M_w = 490$  KDa.<sup>28</sup> To synthesize HAADH, 0.5 g of HA (1.25 mmol) was dissolved in doubly distilled (dd) H<sub>2</sub>O to make a 5 mg/mL solution. To this solution was added a 30-fold molar excess of ADH. The pH of the reaction mixture was adjusted to 6.8 with 0.1 M NaOH and 0.1 M HCl. A 0.78 g sample of EDC (5 mmol) and 0.77 g of HOBt (5 mmol) were dissolved in DMSO/H<sub>2</sub>O (1:1 (v/v), 5 mL each), and the resulting solution was added to the reaction mixture. The pH of the solution was adjusted to 6.8 and was maintained by adding 0.1 M HCl for at least 4 h. The reaction was allowed to proceed overnight. The pH was subsequently adjusted to 7.0 and exhaustively dialyzed (MWCO 10000, Spectra/Por membrane) against H<sub>2</sub>O. NaCl was then added to produce a 5% (w/v) solution, and HAADH was precipitated in ethanol. The precipitate was redissolved in H<sub>2</sub>O and dialyzed again to remove the salt. The purified product was freeze-dried and kept at 4 °C. A 52% ADH incorporation was determined by <sup>1</sup>H NMR spectroscopy (Varian Unity-300).

**Microgel Preparation.** HA-based microgels were prepared by cross-linking two cross-linkable HA (or PEG and HA) derivatives in an inverse emulsion (“inverse emulsion cross-linking technique”). The inverse emulsion was prepared by homogenizing component A (HAADH, 2 mL, 1 or 2 wt % in H<sub>2</sub>O) in mineral oil (50 mL) containing 0.2 mL of Span 80 for 5 min using a Silverson L4R homogenizer (Silverson Machines Ltd., Cheshire, England). Component B (HAALD, 1 wt % in H<sub>2</sub>O, or PEGDiALD, 4 wt % in H<sub>2</sub>O) was then added to the emulsion, which was further homogenized for 5 min. The aqueous phase was allowed to evaporate overnight at 40 °C with constant stirring. Microgels were isolated by precipitation in a large excess of isopropyl alcohol followed by centrifugation to remove the oil phase. The resulting microgels were thoroughly washed with isopropyl alcohol, hexane, and acetone before being dried under vacuum at room temperature. The average diameters of the microgels were determined using a Coulter Counter Multisizer 3 (Beckman Coulter, The Netherlands) with a 100  $\mu$ m orifice.

**Microgel Characterization. Swelling Ratio.** The swelling ratio of microgel preparations was determined gravimetrically. The dry microgels were placed in a vial with known weight, and the dry weight ( $W_d$ ) was measured. They were subsequently allowed to swell in phosphate-buffered saline (PBS; pH 7.4) at 37 °C for 1 h. Upon removal of excess PBS after centrifugation, the wet weight ( $W_s$ ) was determined. The equilibrium swelling ratio (SR) was defined as the ratio of  $W_s$  to  $W_d$ . The results are expressed as the mean  $\pm$  standard deviation for five replicates.

**Enzymatic Degradation.** HA-based microgels were incubated in an HAase solution (100 U/mL in PBS) with a concentration of 2 mg/mL at 37 °C with mild mixing. Fresh enzyme solution was replaced every other day. The time for complete dissolution of hydrogel particles was noted.

**Morphology.** Microgels were attached to specimen stubs using double-coated tape and sputter coated with gold–palladium (100 Å thick). The specimens were imaged with a JEOL JSM 6320 FV scanning electron microscope (JEOL USA, Inc., Peabody, MA) using a 1.5 kV accelerating voltage at a 5 mm working distance.

**Cell Cytotoxicity.** Porcine laryngeal fibroblasts were isolated from the LP of 6–12 month old pigs.<sup>30</sup> Primary tissue explants were cultured in Dulbecco's modified Eagle's medium (DMEM) supplemented with

**Table 1.** Feed Compositions of HA-Based Microgels and Their Properties

sample code	composition (in feed)				$V_A/V_B^c$	SR <sup>d</sup>	$D^e$ ( $\mu\text{m}$ )	$T^f$ (days)
	A <sup>a</sup>	[A] <sup>b</sup> (%)	B	[B] <sup>b</sup> (%)				
MS-1	HAADH	1	PEGDiALD	4	2/1.06	15.7 (0.1)	12.56 (9.58)	3
MS-2	HAADH	2	PEGDiALD	4	2/2.13	20.0 (3.5)	10.20 (4.79)	3
MS-3	HAADH	1	HAALD16	1	2/2	9.7 (1.4)	10.80 (4.82)	32
MS-4	HAADH	1	HAALD39	1	2/2	7.1 (0.3)	10.71 (3.98)	35
MS-5	HAADH	1	HAALD70	1	2/2	5.0 (1.4)	10.73 (3.66)	>35

<sup>a</sup> HAADH, 52% hydrazide content,  $M_w = 360$  KDa.<sup>28</sup> <sup>b</sup> Concentration (w/v) in water. <sup>c</sup> Volume ratio in the feed. <sup>d</sup> Swelling ratio ( $\pm$ standard deviation). <sup>e</sup> Mean particle size ( $\pm$ standard deviation). <sup>f</sup> Time for complete degradation in 100 U/mL HAase solution.

10% calf serum and 1% penicillin–streptomycin without disturbance for one week. The tissue samples were subsequently removed, and fibroblasts that migrated out of the explants were allowed to grow to confluence. Confluent cells were subjected to subculture until passage four. Cells were subsequently trypsinized and seeded into 24-well plates at a density of 40,000 cells/well in 1 mL of culture medium. Microgels were diluted with culture medium and added to each well with the final concentration in the range of 0.002–2.0 mg/mL (three repeats for each sample). The relative toxicity of the microgels to the vocal fold fibroblasts was assessed with a commercially available MTT viability assay kit after 3 days of culture without changing the medium. The solution absorbance was read at 570 nm after the microgels were removed. Parallel assays were carried out to assess the relative cytotoxicity of the corresponding components (HAALD, PEGDiALD, and HAADH) within the same concentration range. Cells cultured under the same conditions in pure medium were used as the control. Results are expressed as the measured absorbance normalized to the absorbance of the control sample. Statistical analysis was performed using a two-tailed Student's *t* test with a *p* value of 0.05 for statistical significance. All values are reported as the mean  $\pm$  standard error of the mean.

**Further Modifications. LY Conjugation.** Microgels (4 mg) were suspended in 1 mL of PBS followed by a slow addition of LY solution (40  $\mu\text{L}$ , 1 mg/mL in PBS). The reaction was allowed to proceed in the dark at room temperature for 2 h with constant rotation. The LY-conjugated microgels were purified by centrifugation and repeated washing with PBS before being analyzed by flow cytometry (FACScan, Becton Dickinson).

**Formation of DXNs.** Dry microgel samples (4 mg) were dispersed in HAADH (0.2 mL, 0.5 wt % in  $\text{H}_2\text{O}$ ) by brief sonication, and the mixture was thoroughly mixed by passing it several times between two syringes connected by a two-way valve. Half of the samples were further mixed with an equal amount of HAALD70 (0.5 wt % in  $\text{H}_2\text{O}$ ). Gels were incubated overnight at 37 °C before mechanical measurements. Macro gels thus synthesized were referred to as DXN(A, MS-*x*), DXN-(B, MS-*x*), and DXN(A + B, MS-*x*), with A and B representing HAADH and HAALD70, respectively, and *x* indicating the particular microgel preparation as summarized in Table 1.

**Preparation of Vocal Fold Tissue Samples.** Vocal fold tissue samples were obtained immediately postmortem from the New England Medical Center (Boston, MA) according to the guidelines of their animal care committee. All specimens were obtained from healthy female canine, 1–2 years old, with an average weight of 24–25 kg. Each specimen was snap-frozen with liquid nitrogen and stored at –80 °C. Sample specimens were thawed rapidly to 37 °C prior to the mechanical tests. For each excised specimen, a circular disk from the midmembrane portion of each vocal fold was removed using a 5 mm dermal punch. The underlying muscle layer and the epithelium were carefully dissected from the specimen, leaving a lamina propria disk for mechanical evaluations.

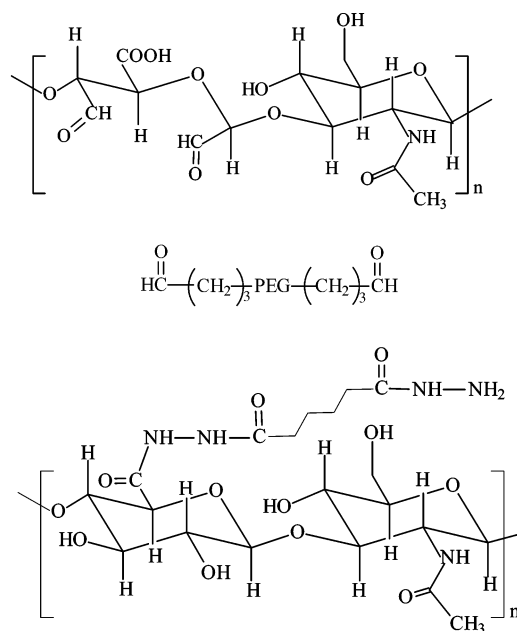
**Mechanical Evaluations.** The mechanical properties of the hydrogel and tissue samples were evaluated using a high-frequency galvanometer in combination with a mathematical model for torsional wave propagation.<sup>31</sup> Specifically, a thin cylindrical sample is placed between two hexagonal plates. The bottom plate is rotated back and forth (less than

$\pm 0.2^\circ$ ) by means of a galvanometer at frequencies up to 2500 Hz. The rotations of the top and bottom plates are monitored by an optical lever technique in which laser beams, reflected off aluminized faces of the hexagonal plates, are passed through a spherical lens, a cylindrical lens, and a butterfly-shaped mask before being captured by photodiode detectors. The output of each photodiode is designed to be proportional to the angular rotation of the respective plate. The rotation of the bottom plate is driven by a computer-controlled frequency generator that steps through a sequence of frequencies. At each frequency the average amplitude of the rotation of each plate is obtained. The experimentally determined amplification factor is obtained as the ratio of the amplitude of the rotation of the top plate to that of the bottom plate. Calibration differences between the recorded outputs for the two plates are accounted for by adjusting the experimentally determined amplification factor to approach the required value of unity as the frequency goes to zero. Amplification factors for each frequency, determined from the experimental records, are compared with those predicted by the viscoelasticity model. For that model, the viscoelastic description of the material is expressed in terms of the amplitude of the complex shear modulus,  $|G^*(\omega)|$ , and the loss angle,  $\delta(\omega)$ . The height and diameter of the sample, required for the wave analysis, are obtained from digital images of the sample in place. The output signal shows a peak in the amplification factor at frequency  $f_{\text{peak}}$ . For each test, a constant modulus  $|G^*|$  and phase shift  $\delta$  are obtained that provide the best fit between the model and the experimental results over a range of frequencies spanning the frequency  $f_{\text{peak}}$ . Data reported are representative values from two consecutive measurements that gave perfectly overlapped resonance peaks.

## Results and Discussion

**Preparation and Characterization of HA Microgels.** Our method for preparing HA microgels relies on in situ cross-linking of HA with built-in cross-linking moieties. Here, chemical modifications were employed to selectively introduce complementary reactive groups including aldehyde and hydrazide to HA (Scheme 1). Specifically, electrophilic bisaldehyde functionalities were generated from the vicinal secondary alcohol on HA by oxidation with sodium periodate.<sup>27,28</sup> This chemistry is a standard method for chemical activation of glycoproteins for affinity immobilization,<sup>32</sup> conversion to a fluorescent probe,<sup>33</sup> or formation of protein–protein conjugates.<sup>34</sup> The degree of oxidation was controlled by the mole equivalent of sodium periodate used in each reaction. In our study, 25%, 50%, and 100% mole equivalents of sodium periodate were used to generate HAALD with 16% (HAALD16), 39% (HAALD39), and 70% (HAALD70) dialdehyde, respectively. A separate modification scheme was applied to impart hydrazide functionality to HA. Thorough purification including repeated dialysis and precipitation was applied to obtain HAADH that is free of active reagents. Figure 1 shows the NMR spectrum of HAADH. The degree of modification was determined by comparison of the integration of the methylene protons

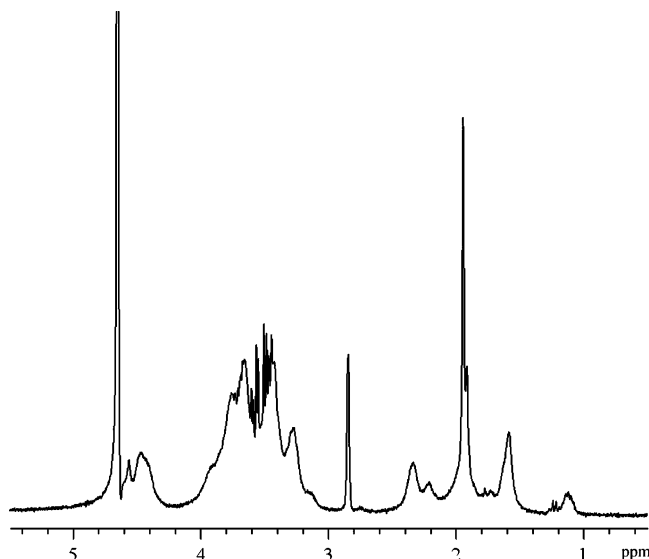


**Scheme 1.** Chemical Structures of HAALD, PEGDiALD, and HAADH

of ADH (2.2–2.4 ppm) with that of the acetamido moiety of the *N*-acetyl-D-glucosamine residue of HA (1.9 ppm), which indicated a 52% coupling of ADH to the HA sugar unit (molar percentage of ADH in every repeating unit of HA). Macroscopic gel formed in less than 30 s upon mixing of 1 wt % aqueous solutions of HAALD70 and HAADH, releasing H<sub>2</sub>O as the only byproduct. When the cross-linking was carried out within the microemulsions, microgels with controlled cross-linking degree and particle size were generated. To facilitate further cross-linking, water was allowed to evaporate overnight. Span 80 was chosen as a surfactant to stabilize the microemulsion as it is FDA approved for human use and has been used for the preparation of microgels targeted for therapeutic applications.<sup>35</sup>

Table 1 summarizes basic properties of HA-based microgels prepared using different feed compositions. In addition to HAALD, we also used PEGDiALD (MW = 3400) as component B to obtain hydrogel microspheres (MS-1 and MS-2) with a wider range of degradation profiles. The relative amounts of PEGDiALD and HAADH in each preparation were chosen to provide equal molar ratios of aldehyde and hydrazide groups in the feed for MS-1 and -2. Both microgels made from PEGDiALD degrade within 3 days in 100 U/mL hyaluronidase, whereas those prepared using HAALD (MS-3, -4, and -5) last more than 30 days under the same conditions. It is also noticeable that MS-1 and MS-2 show higher swelling ratios than MS-3, -4, and -5. We speculate that MS-1 and -2 degraded faster because the cross-linking density of the gel matrix is relatively low, which may be attributed to the following facts. First, PEGDiALD has a maximum of two aldehyde groups per polymer chain, while HAALD has multiple aldehyde groups per molecule. Second, PEGDiALD is amphiphilic, and therefore, a significant fraction of PEGDiALD may have partitioned at the water–oil interface, resulting in a low internal concentration of aldehyde groups.

Comparing MS-3, -4, and -5, we note that microgels made with higher aldehyde content are more resistant to enzymatic degradation. It is worth mentioning that a macroscopic gel made by directly mixing solutions of HAALD70 (1 wt % in H<sub>2</sub>O) and HAADH (1 wt % in H<sub>2</sub>O) degrades readily overnight under the same conditions. These observations indicate that microgels

**Figure 1.** <sup>1</sup>H NMR spectrum of HAADH in D<sub>2</sub>O.

have a higher cross-linking degree than their corresponding macroscopic gels because the concentrations of two cross-linkable components in the microenvironment increase over time with solvent (water) evaporation. However, we cannot exclude the possibility that the presence of residual Span 80 on the microgel surfaces may limit the accessibility of HAase.

All microgels are obtained as fine powders that are easily dispersed when exposed to water. MS-2 appears as a white powder, while others exhibit a yellow tint. Figure 2 shows typical scanning electron micrographs of HA microgels with an average size of approximately 10 μm. MS-1 and MS-2 exhibit relatively less-defined shapes and rugged surfaces (MS-2 in particular). In this regard, we note that the initial feed concentrations in the microemulsion are 20.4 and 30.3 mg/mL for MS-1 and MS-2, respectively, relatively higher than those in MS-3, -4, and -5 (10 mg/mL). Higher concentrations could have increased the viscosity of the microemulsions, which leads to less effective emulsification. The amphiphilic character of PEGDiALD also contributes to decreased stability of the microemulsions. In contrast, MS-3, -4, and -5 were well-defined spheres with smooth surfaces irrespective of the aldehyde content in the composition. The cracks seen on their surfaces appear to be imaging artifacts.

In vitro cell cytotoxicity study is the first step in evaluating the potentials of the HA-based microgels for vocal fold regeneration. The most important cell type in the vocal fold lamina propria is the fibroblast, which maintains the extracellular matrix.<sup>36</sup> It has been shown that porcine vocal folds exhibit anatomy, dimensions, and mechanical properties similar to those of human vocal folds.<sup>37</sup> Cell viability was assessed with an MTT assay using porcine vocal fold fibroblasts that were in direct contact with the microgels. Figure 3 shows the relative viability of vocal fold fibroblasts after incubation with HA-based microgels for 3 days as a function of microgel concentration. The presence of MS-1 and -2 in concentrations varying from 0.002 to 0.2 mg/mL did not elicit any adverse effect on the cultured vocal fold fibroblasts. However, a dramatic decrease ( $p < 0.01$ ) in cell viability was observed when the fibroblasts were exposed to MS-1 or MS-2 at 2 mg/mL. In contrast, MS-3, -4, and -5 were well-tolerated by the vocal fold fibroblasts at all concentrations examined. A microscopic examination (data not shown) indicated that, at 2 mg/mL, the cell monolayer was covered with closely packed microgels. One might expect a decrease in cell viability due to the associated decrease in

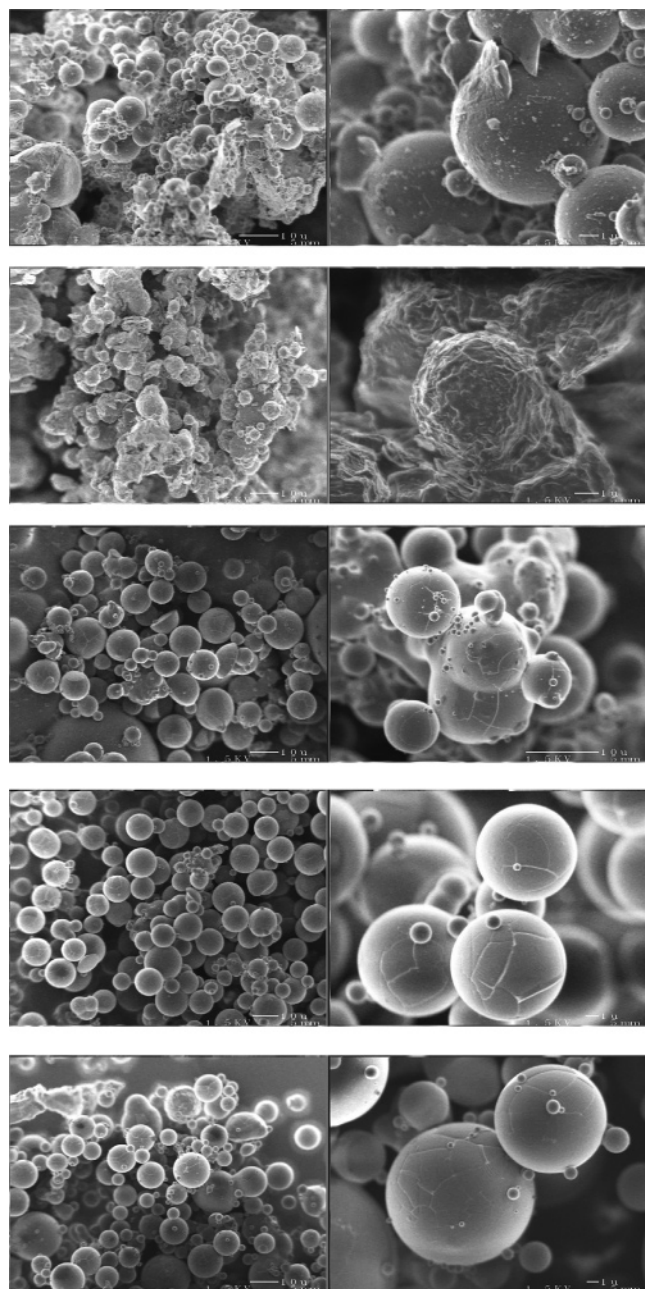


**Figure 2.** Scanning electron micrograph of HA-based microgels at different magnifications. From top to bottom: MS-1, -2, -3, -4, and -5.

nutrients and wastes to be exchanged between the cultured cells and the surrounding medium. Remarkably, even under this condition, MS-3, -4, and -5 do not seem to cause any adverse effects on the cultured cells, whereas compromised cell viability was seen for MS-1 and -2 under the same concentration. These results suggest that the types of polymers used in microgel preparation may play a role in contributing to the observed cytotoxicity.

Cell viability was also assessed in the presence of the corresponding components (HAALD, PEGDiALD, and HAADH), with concentrations varying from 0.002 to 2 mg/mL (Figure 3). HAALD with varying degrees of oxidation are well-tolerated by vocal fold fibroblasts at all concentrations. Bulpitt et al.<sup>27</sup> systematically evaluated the *in vivo* biocompatibility of HA hydrogels based on HAADH cross-linked with various aldehydes, including glutaraldehyde, dextran aldehyde (dextran-ALD), and HAALD. While hydrogels based on HAADH cross-

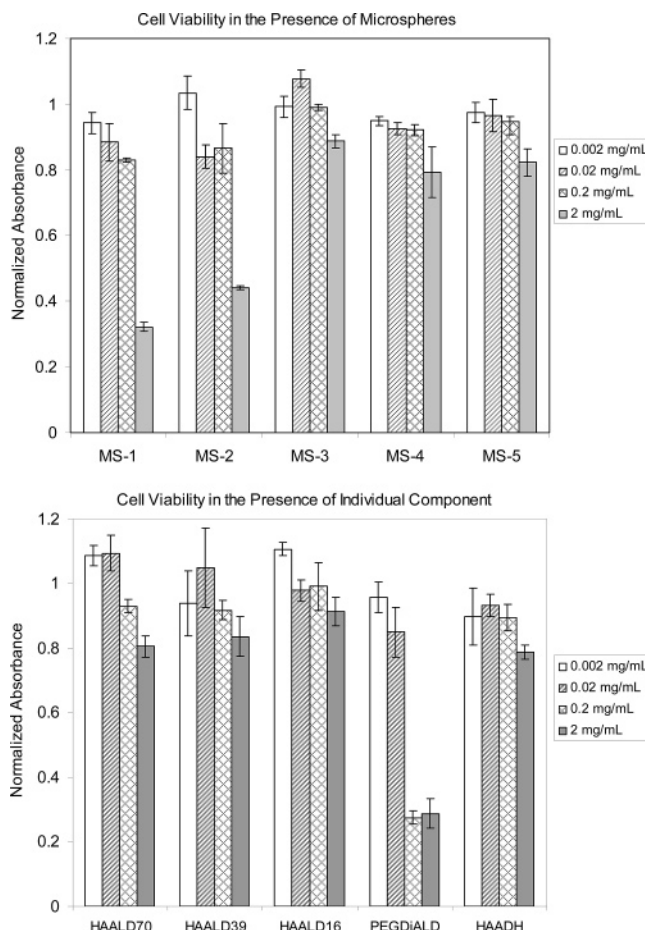


**Figure 3.** Viability of vocal fold fibroblasts cultured for 3 days in the presence of microgels (top) and the corresponding components (bottom) as measured by an MTT viability assay.

linked by HAALD were well tolerated, hydrogels based on HAADH cross-linked by glutaraldehyde and dextran-ALD led to foreign body giant cell reactions indicative of chronic inflammation reactions. The aldehyde group is potentially toxic because it readily reacts with electron-rich functional groups in biological macromolecules.<sup>38</sup> The fact that HAALD is more biocompatible than dextran-ALD suggests that the characteristics of the polymer backbone that carries the aldehyde group play an important role in determining its biocompatibility. With its abundant negative charges on the repeating unit, the highly hydrophilic HAALDs exhibit much reduced reactivity, which is demonstrated by our results. On the other hand, the amphiphilic character of PEGDiALD is likely to promote its association with cell membranes, facilitating the reaction of aldehyde groups toward their surrounding biological entities. As discussed above, the amphiphilic characteristics of PEGDiALD also led to microgels with PEG preferentially anchored to their surfaces, exposing the toxic aldehyde to the surrounding cells. In summary, our *in vitro* cytotoxicity studies indicate that microgels based on HAADH and HAALD have little cytotoxicity toward vocal fold fibroblasts.

**Further Modification of HA Microgels.** Unlike most biodegradable microspheres that are chemically inert,<sup>39</sup> the HA microgels synthesized in our study have residual functional groups that allow for bioconjugation of therapeutic reagents.

**Lucifer yellow-Conjugated HA Microgels.** We are interested in utilizing HA-based microgels for treatment of vocal fold scarring, not just as an inert filler material, but instead as smart entities that can actively remodel the scar tissue. For this

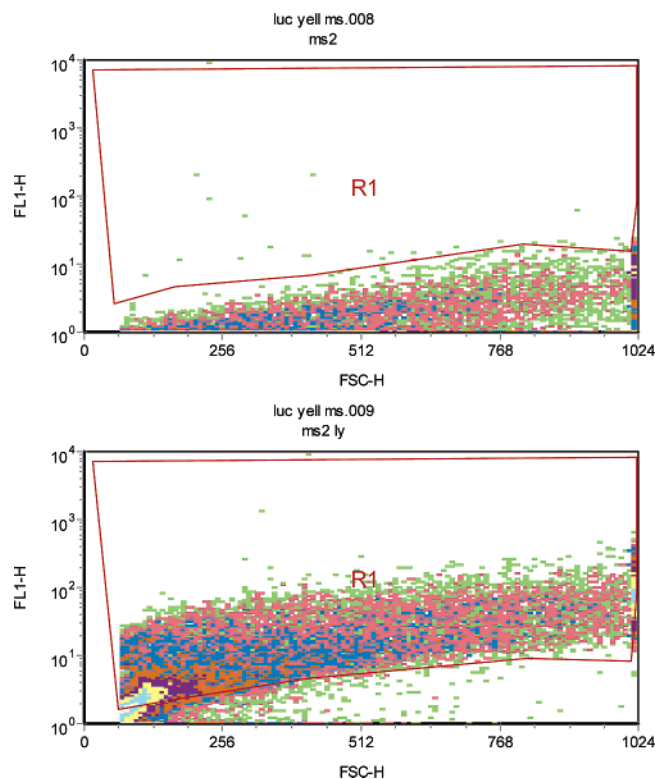


**Figure 4.** Dot plots of fluorescence intensity vs forward scatter for MS-2 before (top) and after (bottom) LY conjugation.

purpose, controlled release of pharmaceutically active compounds can be achieved through their anchorage at predetermined locales of the particulate hydrogel system. To demonstrate the utility and versatility of the microgels for drug immobilization, we have employed LY as the model compound for covalent conjugation. LY is a water-soluble fluorescent dye containing a carbohydrazide functional group that conjugates selectively to aldehydes through the formation of an acid-labile hydrozone bond.<sup>40</sup> Conjugations of the fluorescent dye were performed for microgels of different formulations, and the covalent attachment was verified by flow cytometry. An increase in fluorescence intensity was observed for MS-2 upon LY conjugation (Figure 4), clearly indicating the accessibility of residual aldehyde groups on the microgels. Unfortunately, the slight yellow tint associated with other microgel preparations interfered with the fluorescence quantification of conjugated LY.

**DXNs.** The presence of residual functional groups not only provides reactive handles for chemical conjugation, but also offers opportunities to introduce a second network, giving rise to a DXN with tunable viscoelasticity. To this end, microgels were dispersed in a dilute solution containing HAADH (A, 52% hydrazide) or HAALD70 (B, 70% dialdehyde) or a mixture of both (A + B), and the resulting macrogels were referred to as DXN(A, MS-*x*), DXN(B, MS-*x*), or DXN(A + B, MS-*x*), respectively. Macroscopic gels with interlocked hierarchical organizations form through chemical reactions between the functional groups on microgel surfaces and those in the solution phase. There are two levels of cross-linking in these DXNs: the primary network consisting of cross-linked polymer chains inside each microgel and the secondary network interconnecting the microgels (Figure 5).

Upon mixing with the 0.5 wt % HAADH solution, all microgel preparations led to self-supporting macroscopic gels within 30 min, with the rate of gelation following a particular order: MS-2 > MS-5 > MS-1 > MS-3 > MS-4. On the other hand, upon mixing with the 0.5 wt % HAALD70 solution, MS-2

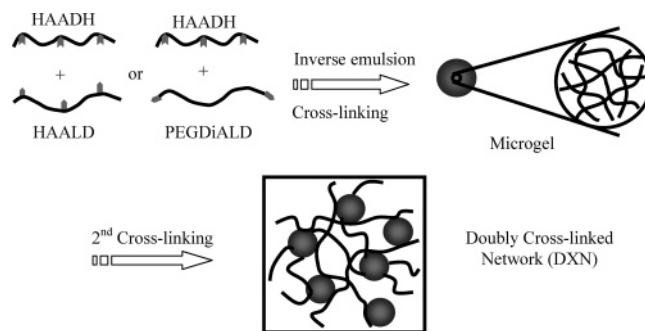


**Figure 5.** Schematic illustration of the formation of microgels and DXNs.

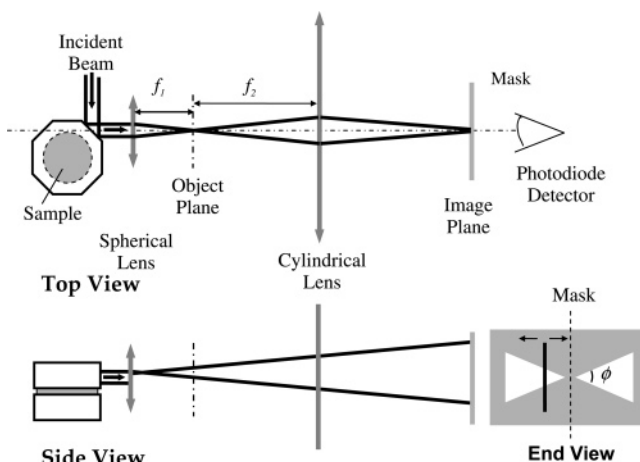


**Figure 6.** Optical layout for torsional wave experiments.

and MS-5 did not form macroscopic gels even with prolonged incubation overnight at 37 °C, whereas other microgel formulations gave rise to macroscopic gels after overnight incubation. These observations suggest that MS-2 and MS-5 have relatively higher amounts of aldehyde groups and lower amounts of hydrazide groups on their surfaces than other microgel formulations.

**Mechanical Evaluation.** As a further measure of the applicability of HA-based microgels and DXNs for vocal fold regeneration, their high-frequency mechanical responses were measured using a torsional wave apparatus in combination with theoretical calculations. It is critical to measure mechanical responses at phonation frequencies because mechanical properties of both the natural tissue and the candidate replacement materials are viscoelastic, or frequency dependent. Rheometers commonly used for measuring the response of viscoelastic materials are limited to frequencies of approximately 10–15 Hz when applied to materials as soft as LP.<sup>41,42</sup> Furthermore, this limitation is not overcome by attempting to redesign a rheometer for higher frequency because these materials are so soft, and consequently have such low wave speeds, that the state of stress and deformation is not uniform throughout the thickness of the sample at the frequencies of interest.<sup>43</sup> Therefore, their mechanical responses at phonation frequencies need to be viewed as involving the propagation of stress waves through the sample. We have recently designed and validated a novel instrument that is capable of measuring viscoelastic responses of both LP tissue and injectable hydrogels at phonation frequencies. Figure 6 depicts the optical layout for this experiment.<sup>31</sup>

There are several indications of the accuracy and reliability of torsional wave experiments. First, repeat tests on the same samples yield essentially the same results for the viscoelastic



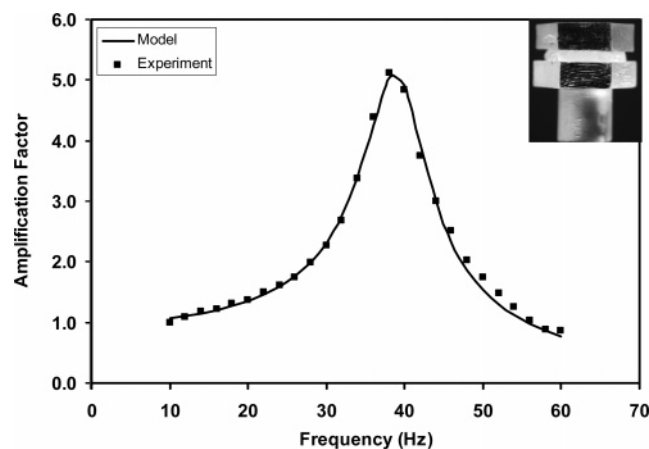


**Figure 7.** Frequency dependence of amplification factors for DXN-(A, MS-4). Best-fit models are shown as solid curves; experimental results are shown as symbols. The inset shows the test sample between the two plates of the loading system.

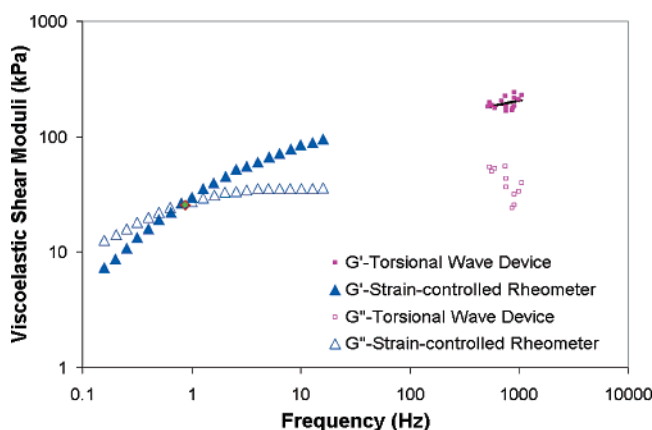


**Figure 8.** Torsional wave measurements of the high-frequency viscoelastic response of silicone putty (PDMS). Low-frequency results from a strain-controlled rheometer obtained by Chan et al.<sup>44</sup> are included for comparison.

moduli. Second, as described in the experimental section, the torsional wave approach determines the amplification factor and the phase angle near a resonance frequency, assuming that the rheological properties of the test samples depend weakly on frequency for frequencies within the resonance peak. Amplification factors obtained for each frequency have been compared with those predicted by a simulation of the experiment based on a torsional wave solution for a linear viscoelastic material. Close agreement between the results of the experiment and the predictions of the model for constant values of the viscoelastic parameters suggests the validity of the model and the relatively weak dependence of these parameters on frequency over a range of frequencies comparable to the widths of the peaks (Figure 7). All torsional wave experiments reported here were conducted in air at room temperature. Samples were tested within a few minutes after their preparation to minimize the drying of the samples at the relative humidity of the room. These precautions have been adequate, enabling qualitative comparisons of various preparations. Third, experiments on a reference material (a silicone putty) commonly used to evaluate the reliability of rheometers have shown (Figure 8) that the viscoelastic moduli measured at high frequencies in our torsional wave experiments are consistent with trends found by others at lower frequencies where conventional rheometers are applicable.

Fully swollen microgels were subjected to the high-frequency mechanical evaluations upon removal of excess water. No

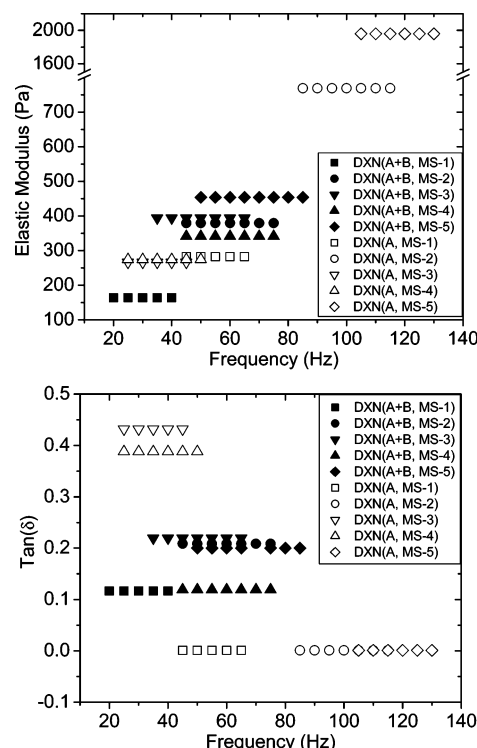


**Figure 9.** High-frequency shearing responses of doubly cross-linked networks based on DXN(A, MS-*x*) and DXN(A + B, MS-*x*): top, elastic modulus as a function of frequency; bottom,  $\tan(\delta)$  as a function of frequency; A = HAADH; B = HAALD70.

obvious resonance peak was observed during a frequency sweep from 10 to 2500 Hz. A very broad peak—well above 100 Hz with an amplification factor of less than 2.5—was present in some cases. However, the amplification appears to be too small to qualify as a resonance peak. Thus, we conclude that microgels by themselves do not have any measurable mechanical integrity.

On the other hand, DXNs described above showed well-defined resonance peaks under the same experimental conditions. Representative values of the inferred storage moduli and the loss measure,  $\tan(\delta)$ , for DXN(A, MS-*x*) are shown as open symbols in Figure 9. The extent of the horizontal lines indicates the frequency range over which the best-fit model provides very good agreement with the measured amplification factors. The data agree with our visual observation of the gelation rates for different DXN(A, MS-*x*) macrogels. While DXN(A, MS-*x*) macrogels based on MS-1, -3, and -4 exhibit similar elastic moduli at frequencies around 30–70 Hz, cross-linking of MS-2 with HAADH led to stiffer hydrogels with elastic moduli around 769 Pa and resonance peaks spanning the frequency range of 85–115 Hz. Mixing of MS-5 and HAADH gave rise to a macrogel with the highest elastic modulus (1959 Pa at frequencies around 120 Hz). It should be emphasized that the exact position of the resonance peak is directly associated with the sample geometry as well as its inherent elasticity. The viscous component of DXN(A, MS-*x*) is expressed as  $\tan(\delta)$ , where  $\delta$  is the loss angle. Interestingly, cross-linking of MS-1, -2, and -5 with HAADH led to highly elastic DXNs with a low loss angle, indicating little energy dissipation during shear. On the other hand, cross-linking of MS-3 and MS-4 with HAADH results in DXNs with a higher  $\tan(\delta)$ . Generally speaking, DXN-(A, MS-*x*) macrogels with a lower elastic modulus usually exhibit a higher loss angle, with the exception of MS-1. Our results suggest that the rheological properties of DXNs are related to the primary network within the macrogels.

The mechanical properties of DXNs can be further adjusted by altering the secondary network between the microgels. Microgels of different formulations were sequentially mixed with HAADH and HAALD70 of equal volume and concentration. Representative values of the inferred storage moduli and the loss measure  $\tan(\delta)$  for DXN(A + B, MS-*x*) are shown as closed symbols in Figure 9. While DXN(A + B, MS-1) has the lowest elastic modulus (163 Pa, 20–40 Hz), the highest value (454 Pa, 50–85 Hz) was inferred from DXN(A + B, MS-5). The elastic moduli for DXN(A + B, MS-*x*) synthesized from MS-2, -3, and -4 are intermediate. Comparable  $\tan(\delta)$  values were obtained for DXN(A + B, MS-1) and DXN(A + B, MS-4), while other compositions are equally more viscous. It is readily noticeable by comparing that the addition of another cross-linking network to the existing macrogels composed of HAADH/MS-*x* does not necessarily lead to an increase in the elastic modulus. For MS-1, -2, and -5, there is obviously a decrease in modulus upon introduction of HAALD70, while the opposite was seen for DXN(A + B, MS-*x*) based on MS-3 and -4. The observed changes in elastic moduli were accompanied by altered  $\tan(\delta)$  values. These results may be attributed to the relative amount of hydrazide groups in DXN(A, MS-*x*) that are available for subsequent cross-linking with HAALD70. Due to the relatively large number of aldehyde groups on their surfaces, MS-1, -2, and -5 consume most HAADH in the formation of DXN(A, MS-*x*), leaving few hydrazide groups in the solution phase available for HAALD70. In addition, the hydrazide groups on the microgel surfaces are not readily accessible for HAALD70 due to the presence of a secondary network formed by HAADH. Therefore, in these cases, HAALD70 is not readily involved in further cross-linking of the secondary network, but only diluting the existing network. As a result, the viscous component of the network is expected to increase as confirmed by our experiments.

For vocal fold regeneration, it is of critical importance that the materials to be injected exhibit viscoelastic properties similar to those of the targeted natural tissue. In our preliminary studies, we used canine vocal fold lamina propria as a reference tissue. It has been shown that 24 h at room temperature, or up to 1 month of frozen storage, did not affect the vocal fold tissue shear properties significantly.<sup>41</sup> Since we are primarily interested in matching the mechanical properties of the replacement materials to those of the lamina propria, we removed both the muscle and epithelium layers from the lamina propria. Our preliminary data indicate that the presence of an epithelium layer increases the overall tissue stiffness (data not shown). Figure 10 shows the high-frequency rheological properties of canine vocal fold lamina propria. The elastic moduli span the range of 285–485 Pa, while  $\tan(\delta)$  values are usually greater than 0.5, indicating high damping associated with tissue samples. As compared to previous studies<sup>41,44</sup> that measured vocal fold biomechanics at low frequencies (<15 Hz) (using a commercial rheometer, a plate-on-plate geometry, a diameter of 20 mm, and a gap of 0.3 mm), our preliminary results indicate a much smaller elastic modulus and a relatively high damping. We note that vocal tissue preparation for mechanical testing is not standardized; thus, our data are not directly comparable to those of the existing studies. More experiments need to be done before any statistical conclusions can be drawn.

A comparison of the mechanical properties of canine vocal fold LP and the microgel-based DXN measured under similar conditions, however, shows that our preparation leads to tunable elasticity and viscosity that covers the range of the natural tissue. The flexibility of the microgel chemistry allows us to cross-

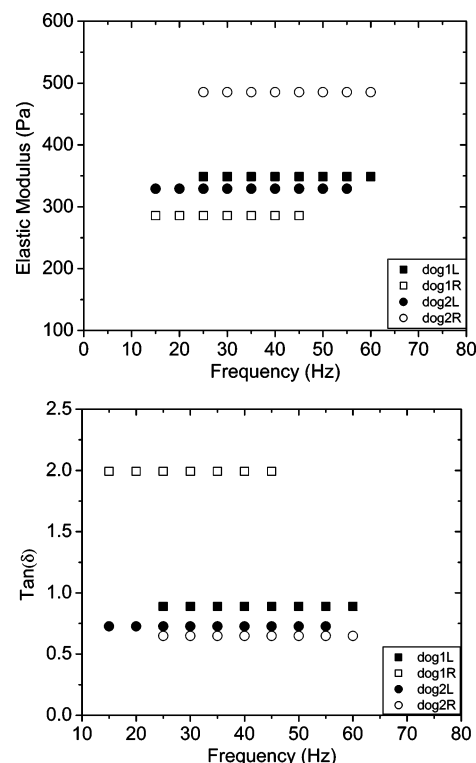


**Figure 10.** High-frequency shearing responses of canine vocal fold lamina propria: top, elastic modulus as a function of frequency; bottom,  $\tan(\delta)$  as a function of frequency; dog1L, LP from the left vocal fold of the first canine sample; dog1R, LP from the right vocal fold of the first canine sample; dog2L, LP from the left vocal fold of the second canine sample; dog2R, LP from the right vocal fold of the second canine sample.

link the microgels with biocompatible polymers that are resistant to enzymatic degradation rather than HA derivatives. In this way, the cross-linking density of the resulting hydrogels can be easily controlled by the secondary cross-linking network, while the enzymatic stability of the system is solely dependent on the microsphere chemistry. Thus, the HA-based microsphere networks appear to be most promising in providing both the low stiffness and the slow degradation that are required for use as simple injection materials.

**Conclusion.** We have investigated HA-based soft hydrogel microspheres (microgels) and cross-linked microgel networks (DXNs) as injectable materials for use in vocal fold restoration. Microgels with diameters around 10  $\mu$ m are synthesized by *in situ* cross-linking of chemically modified HA within inverse emulsion droplets, followed by solvent evaporation. Microgels based on HAADH/HAALD are not only cytocompatible but also resistant to enzymatic degradation. Subsequent cross-linking of the microspheres with soluble HAADH or HAADH followed by HAALD results in hierarchical macrogels with two levels of cross-linking: one within individual microgels and another between them. Torsional wave experiments allow the rheological properties of the DXNs and the natural tissue to be measured at phonation frequencies. The shear modulus and  $\tan(\delta)$  of the networks could be tailored from 164 to 1958 Pa and from 0.001 to 0.43, respectively, by varying the chemical composition of the microgels and the methods used for introducing the second network. The existence of two levels of cross-linking allows the degradation and the mechanical properties of the resulting hydrogel to be adjusted independently. Our preliminary measurements with canine vocal fold tissue suggest that these novel hydrogels hold great potential for vocal fold regeneration



because they can be designed to have viscoelasticity similar to that of the natural tissue.

**Acknowledgment.** This work was generously supported by the Eugene B. Casey Foundation, the Advisory Board Foundation, and the Institute of Laryngology and Voice Restoration. Mechanical testing using the torsional wave experiment was supported by Massachusetts General Hospital and Brown University. We thank Jason Fuller for his help with the flow cytometry.

## References and Notes

- Hirano, M. *Otol. Fukuoka* **1975**, *21*, 239.
- Hirano, M. *ASHA Rep.* **1981**, *11*, 11.
- Titze, I. R. *Principles of Voice Production*; Prentice Hall: Upper Saddle River, NJ, 1994.
- Gray, S.; Hammond, E.; Hanson, D. F. *Ann. Otol., Rhinol., Laryngol.* **1995**, *104*, 13.
- Zeitels, S. M. *Atlas of Phonomicrosurgery and Other Endolaryngeal Procedures for Benign and Malignant Disease*; Singular Publishing Group: San Diego, 2001.
- Bishop, J. *London Edinburgh Philos. Mag. J. Sci.* **1836**.
- Zeitels, S. M.; Healy, G. B. *N. Engl. J. Med.* **2003**, *349*, 882.
- Zeitels, S. M.; Hillman, R. E.; Desloge, R. B.; Mauri, M.; Doyle, P. B. *Ann. Otol., Rhinol., Laryngol.* **2002**, *111*, 21.
- Thibeault, S. L. *Curr. Opin. Otolaryngol. Head Neck Surg.* **2005**, *13*, 148.
- Hirano, S. *Curr. Opin. Otolaryngol. Head Neck Surg.* **2005**, *13*, 143.
- Chan, R. W.; Gray, S. D.; Titze, I. R. *Otolaryngol. Head Neck Surg.* **2001**, *124*, 607.
- Butler, J. E.; Hammond, T. H.; Gray, S. D. *Laryngoscope* **2001**, *11*, 907.
- Gray, S. D.; Titze, I. R.; Chan, R.; Hammond, T. H. *Laryngoscope* **1999**, *109*, 845.
- Lepperdinger, G.; Fehrer, C.; Reitingner, S. Biodegradation of Hyaluronan. In *Chemistry and Biology of Hyaluronan*; Garg, H. G., Hales, C. A., Eds.; Elsevier: Oxford, 2004; p 71.
- Leach, J. B.; Schmidt, C. E. *Biomaterials* **2005**, *26*, 125.
- Arimura, H.; Ouchi, T.; Kishida, A.; Ohya, Y. *J. Biomater. Sci., Polym. Ed.* **2005**, *16*, 1347.
- Hertegard, S.; Hallen, L.; Laurent, C.; Lindstrom, E.; Olofsson, K.; Testad, P.; Dahlqvist, A. *Laryngoscope* **2002**, *112*, 2211.
- Dahlqvist, A.; Garskog, O.; Laurent, C.; Hertegard, S.; Ambrosio, L.; Borzacchiello, A. *Laryngoscope* **2004**, *114*, 138.
- Borzacchiello, A.; Mayol, L.; Garskog, A.; Dahlqvist, A.; Ambrosio, L. *J. Mater. Sci.: Mater. Med.* **2005**, *16*, 553.
- Hansen, J. K.; Thibeault, S. L.; Walsh, J. F.; Shu, X. Z.; Prestwich, G. D. *Ann. Otol., Rhinol., Laryngol.* **2005**, *114*, 662.
- Jia, X.; Burdick, J. A.; Kobler, J.; Clifton, R. J.; Rosowski, J. J.; Zeitels, S. M.; Langer, R. *Macromolecules* **2004**, *37*, 3239.
- Hahn, M. S.; Teply, B. A.; Stevens, M. M.; Zeitels, S. M.; Langer, R. *Biomaterials* **2006**, *27*, 1104.
- Ward, P. D.; Thibeault, S. L.; Gray, S. D. *J. Voice* **2002**, *3*, 303.
- Esposito, E.; Menegatti, E.; Cortesi, R. *Int. J. Pharm.* **2005**, *288*, 35.
- Yun, Y. H.; Goetz, D. J.; Yellen, P.; Chen, W. L. *Biomaterials* **2004**, *25*, 147.
- Bae, K. H.; Yoon, J. J.; Park, T. G. *Biotechnol. Prog.* **2006**, *22*, 297.
- Bulpitt, P.; Aeschlimann, D. *J. Biomed. Mater. Res.* **1999**, *47*, 152.
- Jia, X.; Colombo, G.; Padera, R.; Langer, R.; Kohane, D. S. *Biomaterials* **2004**, *25*, 4797.
- Bouhadir, K. H.; Hausman, D. S.; Mooney, D. J. *Polymer* **1999**, *40*, 3575.
- Freshney, R. I. *Culture of Animal Cells: a Manual of Basic Techniques*; J. Wiley: New York, 2000.
- Clifton, R. J.; Jia, X.; Jiao, T.; Bull, C.; Hahn, M. S. *Proc. IUTAM Symp. Mech. Biol. Tissue* **2006**, 445.
- Xuan, H.; Hage, D. S. *Anal. Biochem.* **2005**, *346*, 300.
- Lee, J. A.; Fortes, P. A. *Biochemistry* **1985**, *24*, 322.
- Dent, A. H.; Aslam, M. The Preparation of Protein-Protein Conjugates. In *Bioconjugation: Protein Coupling Techniques for the Biomedical Sciences*; Aslam, M., Dent, A., Eds.; MacMillan Reference Ltd.: New York, 1999; p 216.
- Murthy, N.; Xu, M.; Schuck, S.; Junisawa, J.; Shastri, N.; Frechet, J. M. J. *Proc. Natl. Acad. Sci. U.S.A.* **2003**, *100*, 4995.
- Catten, M.; Gray, S. D.; Hammond, T. H.; Zhou, R.; Hammond, E. *Otolaryngol. Head Neck Surg.* **1998**, *118*, 663.
- Jiang, J. J.; Raviv, J. R.; Hanson, D. G. *Ann. Otol., Rhinol., Laryngol.* **2001**, *110*, 1120.
- O'Brien, P. J.; Siraki, A. G.; Shangari, N. *Crit. Rev. Toxicol.* **2005**, *35*, 609.
- Keegan, M. E.; Falcone, J. L.; Leung, T. C.; Saltzman, W. M. *Macromolecules* **2004**, *37*, 9779.
- Stewart, W. W. *Nature* **1981**, *292*, 17.
- Chan, R. W.; Tize, I. R. *J. Acoust. Soc. Am.* **1999**, *106*, 2008.
- Chan, R. W.; Titze, I. R. *J. Acoust. Soc. Am.* **2000**, *107*, 565.
- Titze, I. R.; Klemuk, S. A.; Gray, S. *J. Acoust. Soc. Am.* **2004**, *115*, 392.
- Chan, R. W. *J. Acoust. Soc. Am.* **2004**, *115*, 3161.

BM0604956